ARTICLE

Construction of Customized Bio Incubator and Designing of Tailored Scaffolds for Bone Tissue Engineering from Laboratory Scale Up to Clinical Scale

Soliman Abdalla[1,2,*] and Shiref Kandil[2]

[1]Department of Physics, Faculty of Science, King Abdulaziz University, Jeddah, Saudi Arabia

[2]Department of Materials Science, Institute of Graduate Studies and Research, Alexandria University, Alexandria, Egypt

[*]Corresponding Author: Solimann Abdalla. Email: smabdullah@kau.edu.sa

ABSTRACT

In order to obtain larger, clinical-scale and practical-scale bone grafts, we have designed both tailored scaffolds and tailored bio incubator with optimal bio-production characteristics. Using DIC files to Simpleware Scan-IP (Simple-ware-exeter United Kingdom), we have digitally reconstructed segmental additive bone-tissue in order to perform images processing. Both hydroxyapatite and tannin composites have been used in order to get the final bone modules combined for retexturing of segmental bone defect. We have found that sectioning of bone segment deficiency reorganizations into well disk-shaped design permits one to standardize the cell culture and seeding protocol, to get better products. The present study concludes that some techniques with cultured cell in segmental bone grafts in the laboratory can be transferred and clinically used.

Nomenclature

BSs	bone segments
BTE	bone tissue engineering
DIC	computer files and extensions
DICOM	digital imaging and communications in medicine
i-PSCs	induced pluripotent stem cell
NECM	network of extracellular matrix
NECM	network of extracellular matrix (NECM)
PIs	perfusion inserts
RF	rabbit femur
SB	segmental bone
SBGs	segmental bone grafts
μCT	micro computed tomography

1 Introduction

Human bone is a metabolically active tissue accountable for protection, support, locomotion, and mineral storage and it can provide an environment for homeostasis, and hematopoiesis [1,2]. Most remarkably, bone tissues suffer a periodical remodeling [3]. This means keeping a metabolic balance between the osteoblast-mediated bone formation and osteoclast mediated bone metabolic processes throughout the entire period of mammalian-life [4–6]. In general, bone metabolic processes, in adults, takes about ten days and reformation takes about three months (up to 5 months) to reach about 10% of osseous tissue through each year [7–9]. Human bone has an excellent-intuitive repair properties and rehabilitation capability; however, and unfortunately, these properties are valid only for minor damages. However, defects, cracks and/or small fractures (critical size threshold is typically around 2 cm), which exceed the critical size some external techniques and interventions are still needed for the, based on the anatomical site [10–13].

In 2019, the global demand for bone graft substitutes was estimated at over 2 billion USD [14] and is predicted to hit 4.85 billion by 2030, double the current rate [14]. Therefore, an urgent need to develop and ameliorate bio-mimetic-bone grafts (BGs) as several million people worldwide have become witnesses of orthopedic ailments every year [15,16]. Here, bone tissue engineering (BTE) remains the most effective, low cost and promising approach that could mitigate the side effects combined with the typical gold standard techniques [17]. Regardless of the progress of several biomaterials, tannin compositions have received recent attention for their potential use as a smart graft material with stem cells 21 instead 18 [18–24] for creating a hierarchical bone structure.

In the human skeleton, cells are arranged in a very well-recognized microenvironments having some complex network of extracellular matrix (NECM). With some extent of similarity to a beehive, this net not only supports the cells but also supplies chemical, topographical, and mechanical cues arranging the cell fate [25]. Some authors [26,27] have reported that, osteoid-cells have some sort of crystal-structure, however, others have reported dimensions of these osteoid blocks ranging within 10 nm up to 300 nm [28,29]. Several authors have provided certain evidence that the NECM characteristics drastically affect cell morphology, emigration, propagation, differentiation, and discrimination [30–32]. In order to have a capacity to produce good-replicas of bone-NECM in micro-scale (or even in nanoscale), one should study the essential factors that control the bone-NECMs interaction techniques both *in vitro* and with using suitable stem cells and tissues for several biomedical purposes [33]. Authors have used stem cell differentiation, in such a way to mix molecules with some standard plasticity composites used as substrates. This mix cannot supply the cells with the essential electric information: Topographical, and mechanical signals, can exist in the NECM-microenvironment; and these topographical, and mechanical signals are essential factors necessary to control the stem cell vitality and activity to perform complete differentiation into mature cell types [34–36]. Recently, several authors have used bottom-up self-assembly techniques in order to investigate the responses and the biological-behavior of stem cells to certain (particular) topographical variations [37–39]. Moreover, Zhang et al. [40] and Zhou et al. [41] have mixed oligopeptides with active stem cells to form some adhesion motifs; while Amores de Sousa et al. [42] have obtained nanofibers when combining oligopeptides with active stem cells, or combined with hydrogels [43]. This has been used to fabricate surface patterns that mimic tissue characteristics and improve stem cell differentiation [43]. Dellatore et al. [44] have obtained mimic tissue when improving stem cell differentiation. On the other hand, authors in references [21–24] have noticed that addition of tannin composites to a stem cells NECM can ameliorate the cell viability and can provided the NECM-microenvironment with topographical, and mechanical signals, which arise due to the presence of these natural composites through the NECM-microenvironment. Tian et al. [45] have used tannic acid modified hydroxyapatite to evaluate on some definitive-sized calvarial defects in rats. da Câmara et al. [46] have used tannin composites to activate the biocompatibility and cell response, macro-porous cement scaffolds

using polyethylene glycol particles. Koopmann et al. [47] have reviewed some bio-applications of tannin composites. In fact, very reactive polyphenols compounds compose the main trunk of the natural tannin. They are sustainable-bio-sourced, eco-friendly, and low-cost materials. Recently, several authors have been interested to understand the multilateral properties and characteristics of tannin composites [48–69]. In general, tannin compounds can react and interact with a broad set of various compounds, inclusive chalcogenides, and ceramics, as well as some organic classes.

For example, hybrid-systems allow the preparation of different hi-tech nanocomposites. Therefore, these various compounds have some possibility to be used in different technological applications. In addition, the tannin compounds can be used as functional chemical building blocks, in particular in bio- chemical and bio-medical applications. This makes the main aim of the present study: One presents a reproducible, low cost and effective solution to construct segmental grafts, which can be used to repair segmental bone (SB) deficiency, in suitable practical size. In fact, one can effectively treated and repaired the SB deficiencies using BGs techniques, and in general bone engineering (BE) [70–73]. However, in order to obtain clinically applicable production of therapeutically parts, there still some challenges; in particular when repairing (or reproducing) relatively massive parts (exceeding two centimeters) [10]. Therefore, the present study suggests a technique including growing segmental bone grafts (SBGs) in the laboratory. Then, these SBGs can be transferred and clinically used.

From an economic point of view, the economic load of skeletal defects is huge and expected to exponentially increase over the next decades [74,75] due to the fast global population-growth and addendum of life hope [75], with a combined annual US market for bone repair and regeneration therapies projected to reach 3.5 billion by 2017 [76,77]. A large number of bone-proxy composites are nowadays available for skeletal reconstructions, with the transplantation of autologous bone grafts still remaining the gold standard treatment [78]. Cheap three-dimensions printing devices are nowadays available for about five hundred US$, however, these devices bring out lower efficient substitutes, suitable for many applications. In addition, industrial tools cost about thirty thousand of US$; while laser-based devices can make higher efficient outputs (metal-like products) can cost about one million US$. Our proposed technique, with 5k US$, lies in an intermediate range between the industrial tools and the laser-based devices as illustrated in Fig. 1. Note that the cost axe is presented in more convenient logarithmic scale to encounter 500 US$ with 3.5 million US$. Fig. 1 shows that the ratio efficiency/[log (cost)], (R), is the best for our devices. R is estimated after the area under the curve (Fig. 1) of each device/tool. (i) 3D-printed devices R = 5.58, (ii) Industrial tools R = 7.82, (iii) Present device R = 17.57, (iv) Laser-based devices R = 14.97.
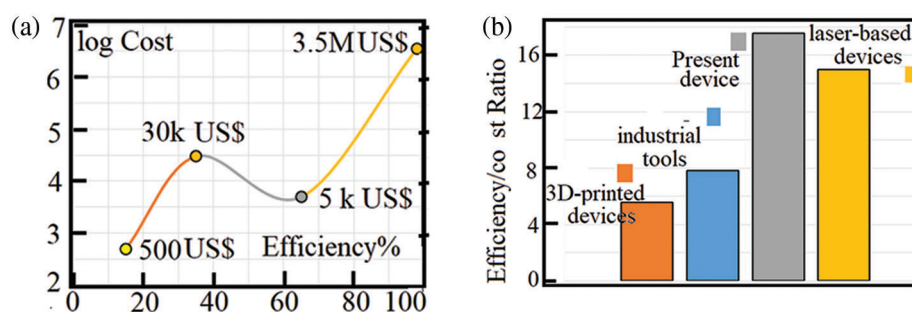

Figure 1: (a) Logarithm of cost as a function of efficiency, (b) Efficiency/cost ratio comparison

From a technical point of view, in order to obtain grafts with relatively large dimensions (more than 3 cm), the present technique can be led to larger grafts compared to other techniques covering their requirements in an easy and effective handling. For example, for larger bone-defects, each tissue chamber could be both isolated and perfused independently to obtain the desired output component. The grafts can

be regulated so that each segment is subjected to comparable shear stress through culture to optimize output-variability.

The main future of the present technique is how to satisfy the need for larger bone segments with (i) uniform seeding of large scaffolds, (ii) under desire anatomically shaped scaffolds, (iii) long distance perfusion of segmental grafts in bio incubators, (iv) customization of bio incubator design and, (v) and highly interest handling-standardization. Therefore, it is censorious to present a novel-devise having controlled-engineering scenarios which have the ability to (i) optimize (minimizing) handling-techniques, (ii) increase output-variability, and (iii) smooth transition of tissue-engineered segmental bone grafts from lab-scale to bed-scale. The present technique has encountered, and even overcome, these challenges by a suitable combination of typical bone-engineering and certain state-of-the-art using tissue-culture- and cell-technology.

2 Materials and Methods

In general, the main experimental details are previously detailed in references [21–24]. We have digitally reconstructed segmental added-on bone-tissue. These SB defects are represented by red regions in Fig. 2a. Then, one has transversally partitioned to the lengthwise direction, which leads to production of parts with well recognized thickness and dimensions (Figs. 2b and 2c). After partition, one has cultured the stem cells in a tailored incubation cell (Fig. 2d). During the culture processes, one has added, in a tailored "bio-mold", both hydroxyapatite and tannin composite [21–24] in order to get the final bone modules combined for retexturing of SB defects.

2.1 Sectioning of SB Defects

One has purchased rabbit femur (RF) from the market, cleaned to get rid of all covered tissues. One has imported DIC files to Simple ware Scan-IP (Simple-ware-exeter United Kingdom) in order to perform images processing, which means that one has created a mask for, just, visualization. Using the finite element module with polishing a masquerade, one can model the RF by interlocking the full model. Using a CAD-computer-aided-design, one has modeled the RF in fourteen RF-segments each of five mm-thick with 200 micrometer thick cylinders. Then, one has isolated the bone segments (BSs) and tailored perfusion inserts (PIs) with de-cellularized BT-scaffolds. The nearest six BSs obtained from sectioning are named work S1–S6, which corresponds to a 3 cm long RF-defect.

2.2 Molds Building, Forming and Manufacturing for Shaping the Perfusion Inserts

In order to produce tailored PI, one has designed molds in AutoCAD (Autodesk, Figs. 3a–3e). In fact, various mold-structures have been examined in order to permit the manufacturing of nearly perfect PI. The three-part design contains a base 1.95 cm in radius, a ring 1.95 outer radius, 1.3 cm inner radius and one cm height, with the ability that the different segments can easily join together. To patch with the simulation data and to form an equalized container through the PI. One has controlled the spline-offset 0.15 cm from the board of each partition, each BS are projected 0.2 cm. At the maximum of the projected issue, one has added a block plug (0.18 cm × 0.18 cm) to control the reconstructed BS to the cast (through an aperture of 0.19 cm × 0.2 cm from the center). Table 1 reports the dimensions of the different perfusion bio incubator parts (Figs. 3a–3e).

2.3 Formation of Tailored Perfusion Inserts

As it is seen in Figs. 2a–2h, one has formed the tailored-PIs through molding using low–molecular weight PDMS (poly di-methyl-siloxane). Then, one has mixed an elastomer (type 184 silicone-elastomer-kit) with a treatment agent DC (Dow Corning, Midland, MI) with a ratio 9:1(w/w).
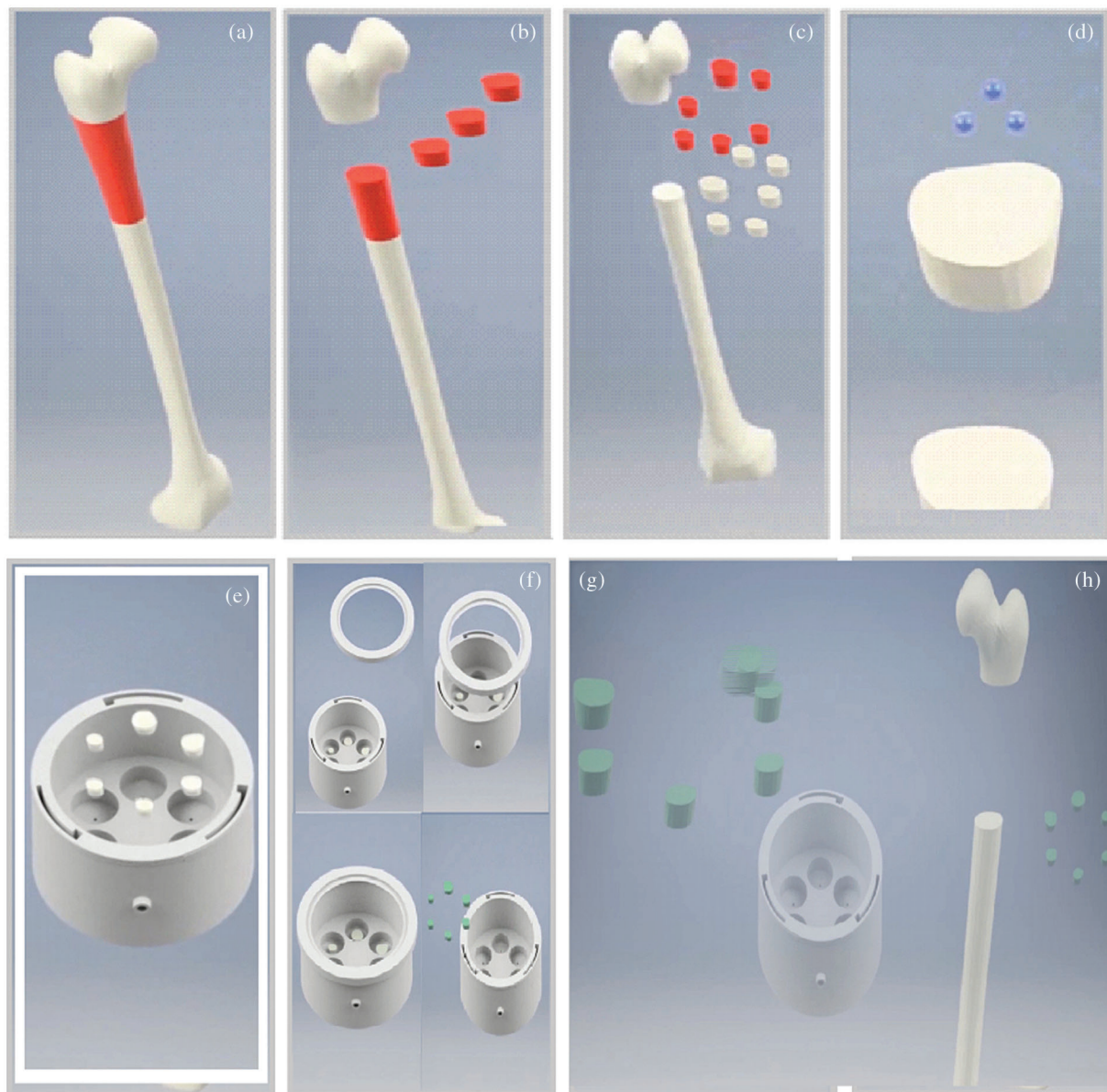
Figure 2: (a) Rabbit femur (white) containing bone-defect (bone segment BS) (red), (b) Sectioning of red, (c) Reconstructions of BSs, (d) Cells (blue) are seeded into the tailored segments, (e) General view of the bio-incubator, (f) Details of the bio-incubator, (g) The tailored scaffolds, (h) The final segments

In order to degas the mix, one has carefully mixed the elastomer base and treatment factor, then has placed the mixture under vacuum. Finally, one has transfused the mix towards the gathered molds, and cured for one hour at sixty degrees centigrade. Following the sufficient temperature reduction and final cleaning, one has contentiously dislocated the PI were from the molds (Figs. 2d and 2e).

2.4 Formation of Tailored Bio-Scaffolds

As it has been detailed in references [21–24] about the formation of decellularized BT-scaffolds. One has sawed forties of trabecular BT from cow logs, from both distal and proximal locations.
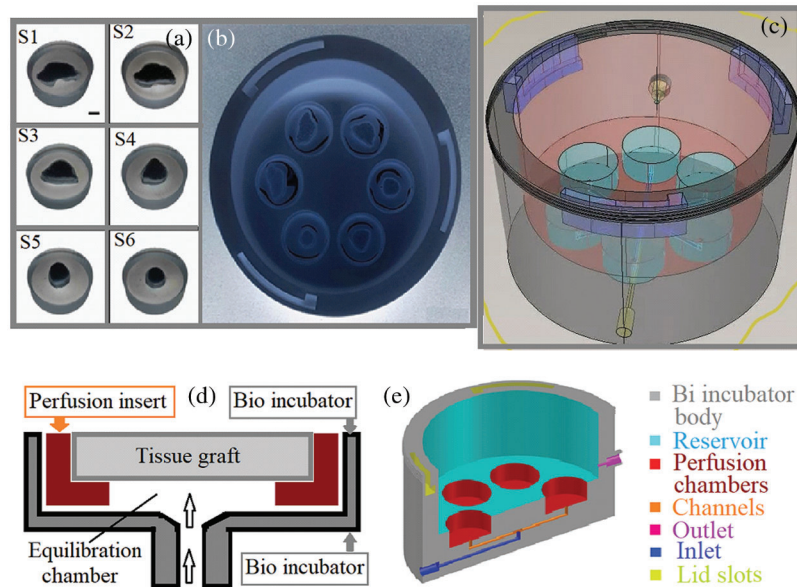
Figure 3: (a) BSs suitable for each 6defect segments located in their corresponding perfusion inserts, (b) Vertical projection of the six BSs, (c) 3-D view of a transection of the bio incubator, (d) 2-D view of a transection of the bio incubator, (e) 3-D field of vision of a transection of the bio incubator

Table 1: Different values of the dc-electrical conductivity σ_{dc}, relaxation time τ, low frequency dielectric constant $\varepsilon'dc$, and the dielectric constant at high-frequency, ε'_{∞}

G_G	τ (280 K)	τ (320 K)	σ_{dc} (280 K)	σ_{dc} 320 K	ε'_{dc} (280 K)	ε'_{dc}320 K	ε'_{∞} 280 K	ε'_{∞} 320 K
0.04591	2.34036E–07	0.000000125	0.402337629	0.714285714	30855128.01	25100	61.97719609	78.1
0.05887	2.68701E-07	0.000000141	0.350431384	0.429184549	32443.47762	26400	95.24043489	79.3
0.07187	2.99379E-07	0.000000153	0.314521793	0.30651341	36147.61529	27700	106.1142286	80.6
0.08487	3.23367E-07	0.000000163	0.291190597	0.238379023	39043.88693	29100	114.6164666	81.9
0.10028	3.52822E-07	0.000000172	0.266880591	0.188679245	42600.37316	30600	125.0568177	83.5
0.11088	3.70043E-07	0.000000177	0.254460659	0.165016502	44679.63051	31700	131.1606969	84.6
0.12388	3.92886E-07	0.000000183	0.239665846	0.143010368	47437.7679	33000	139.2573786	85.9
0.13688	4.11458E-07	0.000000188	0.228848219	0.126182965	49680.14532	34300	145.8400576	87.4

Noting that, before one has started the seeding-processes, all tailored scaffolds have been cleaned and sterilized with ethanol alcohol for 8 h; then they have been located in their corresponding PDMS-room, and finally they have been kept in a standard-conditioned conditions for one complete day.

2.5 Building and Controlling of Bio Incubator

First, one has drawn the perfusion system, which contains the ports, channels and/or manifold, perfusion rooms and storage-location (six cylindrical chambers). Then, one has subtracted the entire perfusion system from an odd coinciding-3D-object. One has drawn a hole on the exterior surface of the reservoir forming both inlet and outlet-ports, which are joined with the main chamber. Fig. 3 shows the details of the bio incubator (Figs. 3a–3e).

2.6 Seeding Processes in Perfusion Bio Incubator

One has assessed and derived iPSCs as it has been previously reported [21–24]. We have expanded the iPSCs in an environment containing strong (10%)-glucose KnockOut Dulbecco's; then one has located each scaffold in its corresponding perfusion insert following sterilization in ethyl alcohol for eight hours.

Following that, we have conditioned the scaffolds in an expansion environment for one day. Then, using autoclaved (Systec Company), one has blot-dried and has cultured with cells using a droplet technique [79]. In order to permit good attachment between cells and scaffolds, one has placed the constructs in a suitable moisturize environments at standard temperature and humidity (37°C and our calibration labs keep a relative humidity environment in the range 30% up to 50% in order to get the most suitable balance) for three hours. One day after, one has collected the expansion medium while one has estimated the number of cells that failed to adhere to the scaffolds using hemo-cytometer. Three days after seeding, one has transferred the scaffolds with their adhered cells to the perfusion bio incubator following seeding, for five weeks in osteogenic environment having high-glucose concentrations. Ending culture-processes, one has perfused the specimens with a suitable rate of flow (not less than three ml/minute and not more than four ml/minute). Then, one has collected the specimens for the following steps.

2.7 Cell-Activity, -Distribution, -Adhesion, and -Growing on Scaffolds

Three days following seeding and five weeks following culture in osteogenic induction environments, one has stained the specimens with FDAfluorescein di-acetate. Then, one has counted the quantity of attached-cells exists in the specimens with PrestoBlueCellViabilityReagent-13261TM. Then, one has estimated the fraction of BT production using: BT = [(Total area−empty area)/Total area] * 100%.

One has estimated the quantity of active-cells exist in the samples when finishing the culture processes by the help of PrestoBlue$^{®}$ assay; here, samples have been handled with six ml of osteogenic-medium havining 10% (by volume) of PrestoBlue$^{®}$ anaytes. They are incubated about two hours at 37°C. Then after, one has measured the fuorescence at the excitation:emission wave length range 560:590 nm. The quantity of viable cells has been presented after the amplitude of intensity of fuorescence.

3 Results and Discussion

3.1 Research-Application Scale Graded Up to a Clinical-One

In order to overcome the difficulties which, arise from large partitions, it is suggested using different techniques: (i) The location of defect can exactly be precised in 3D, or the replacement part as shown in Fig. 2a, (ii) Segmental defects, which are produced by sectioning into modules (6 red segments in Fig. 2b), (iii) Fig. 3b shows selected 13 segments in 3D where their totality is illustrated in Fig. 3c.

On the other hand, checkpoint-startovan© has been used to convert big µCT scans into smaller, manageable and more manipulated files maniple. Big µ-scans can be shrunk into some smaller ones.

We have imported digital imaging and communications in medicine (DICOM) [79] obtained from µCT of decellularized BSs (0.40 cm height and 0.20 cm in radius) in ScanIPSimpleware (Simple'ware) for producing of a three-dimension model and following formation of a transection illustration along the lengthwise-axis. With using Img2 CAD 7.02, we have converted the two-dimension illustrations from PNG up to DWG files, after that, we have imported them in ACAD Autodesk in order to illustrate a sufficiently good replication of the two dimension illustrations with a diameter that corresponds to the size of the largest BS produced from sectioning of the RF (Figs. 3a–3e).

In the different reported techniques of BE [80–104], it is remarked that: It is difficult to jump from a research-application scale up to a clinical-application one. Therefore, some growing SB grafts in the research-application scale (in the laboratories) can be completed with some manipulations. Then, they would be easily converted in the clinical-application scale. Thus, when some digital-reconstructions of

SB-defects into breadths are reconstructed, these challenges would be affected. This can, facilitates the transfer of BE-grafts up to the clinical-application, which is presented in Fig. 2. This sheds the light on the convenience and the ascendancy of the proposed technique (shown in Fig. 2), and can lead to operating methods, which would lead, in turn, to more repeatable and useful techniques of SB grafts.

3.2 Arrangements and Partitions of Defect Reconstruction and Manufacture of PI and Scaffolding

In Fig. 4a, using micro-CT imaging, the RF has been browsed out and has proceeded a SB-graft corresponding to a defect present on this RF. Fig. 4b shows produced-files to simulate a fiddle image of the RF-surface of the bone. Then, the model has been sectioned into separate segments as seen in Figs. 4a–4e. These segments have been, then, used as samples to build different PI and to custom similar scaffolds. The obtained scaffolds have been used as bone-bio-incubators to culture the stem cells in order to form the final samples. We have chosen the thickness of the scaffolds to vary from a minimum value of 5 mm up to a maximum thickness, which confined on the BS-structure and perfusion regime adopted. This means that the BS-thick can be controlled and/or increased to larger values depending on the seeding and culture environment parameters.
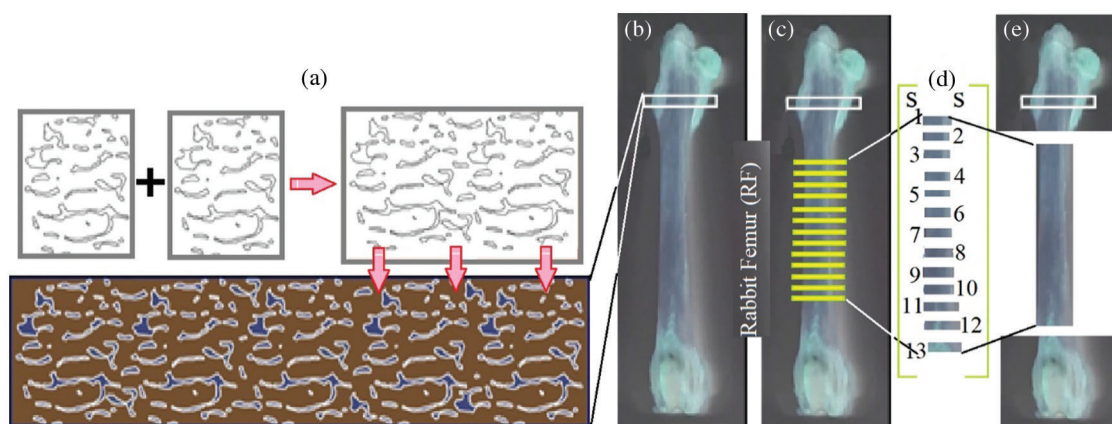

Figure 4: (a) Two-dimension illustration of decellularized bone scaffold, (b) RF, where the examined sections in Fig. (3a) is illustrated, (c) RF where the 13 partitions are illustrated in yellow, (d) Magnification of the yellow partitioned parts, (e) Final situation of the RF

Thus, the compactness of these BS can be controlled by increasing them to greater values with maximizing the seeding and culture factors.

We have used the nearest six BSs obtained from sectioning of the BS-digital restoration, corresponding to a three cm-long RF-defect. According to sectioning, the exterior area of the models of each BS has been corrected in order to obtain three dimensions samples (Fig. 3e). Then, these samples have been utilized to build tailored PI and BSs. In a parallel technique, the digital models of the samples of other bone tissue can be used, including bovine bone scaffolds. In fact, the facility to combine between the architectural-design of biomaterials scaffolds and both perfusion conditions and the seeding protocols can lead to a huge increase of the bone-tissue reproduction in SB engineering applications.

Figs. 4a–4e illustrate the formation of a cross section two-dimension illustrations of BSs for simulation investigations. The 2D illustration, which represents the trabecular design of decellularized BS can be generated by using micro-computed tomography. This has been carried out to generate a larger illustration having dimensions compared to the wider BS (S1), which is the biggest BS in the present work. These have been formed from sectioning of the RF-model.

Unfortunately, a required special bone-bio-incubator is not present in the commercial market, and every case should be built up according to their own bone-bio-incubators, however, these bone-bio-incubator control the supply of a sustained nutrients to cells during the different steps of the culture processes. This increases the possibility of producing a large amount of bone tissues. In fact, tailoring an 'own bone-bio-incubators' with special clinical requirements can meet different difficulties: High cost, long periods of production, and good delivery of bone segments to patients. The necessary conditions to have a good and suitable bone-bio-incubator are the following it should: (i) be self-contained, (ii) be simple design, (iii) have at least one feeding-inlet, (iv) have a system of channels (manifold): For example, in the present work, 6-tissue compartments have been used, each of them corresponds to the number of segments manipulated, (v) have reservoir, (vi) have an outlet, (vii) have a lid for straightforward path, have a monitor to show the culture-procedure processes (Fig. 2e). In order to fulfil the needs of clinical and/or experimental, the diameter of the tissue chamber should be exactly similar to the radius of the PI that holds the BGs in a press-fitted manner to allow straightforward BT-perfusion through seeding growing (Figs. 3a and 3b); thus, both the number of tissue chambers and their capacity to meet the clinical needs can be changed under desire. In addition, in order to bear in mind, the big variations in graft-diameter, the BT-chambers can be perfused in an independent manner and can be isolated. Thus, we can control and regulate the perfusion in order that each segment is subjected to suitable (and not destructive) shear stress through the culture processes.

3.3 Seeding of Cells on Scaffolds and Culture in the Bone-Bio-Incubator

Enormous quantity of cell (some hundreds of millions of cells) should be supplied in order to build blocks of growing segmental skeletal reconstructions (bone-tissue). Sladkova et al. [100] have shown that nuclear-retrograding permits the production of essentially huge numbers of analogous cell-units, which contains the power to discriminate to all of the functional-cells, which constitute the BT [102]; however, the typical techniques to cultivate BGs (in cm scale) use, in general, mesenchymal stem cells obtained from normal BT. The mesenchymal stem cells escalate gently, however, they fast attain agedness. Several authors [103–106] have reported that iPSC may not be sufficiently available in for patients suffering bone-disorders.

In Fig. 5, the down part illustrate the attached cells percentage (seeding efficiency-left) where the measured fluorescence intensity is "560 nm:590 nm" for the six studied segments (S1–S6); here, the gray color stands for static conditions while orange colored data represent the seeding efficiency (percentage of attached cells) carried out at dynamic conditions: Blue colors are with static conditions and the pale green colored data represent the seeding efficiency (percentage of attached cells) carried out at dynamic conditions. The experimental fluorescence intensity taken at wavelength "560 nm:590 nm" for the six studied segments (S1–S6). For more clarifications, the illustrated numbers corresponding to colored squares denote the following: 1: Attached cells percentage (seeding efficiency-left) with static conditions, 2: Attached cells percentage (seeding efficiency-left) with dynamic conditions, 3: Fluorescence intensity "560 nm:590 nm" for the six studied segments (S1–S6) Blue are with static conditions, 4: Fluorescence intensity "560 nm:590 nm" for the six studied segments (S1–S6) pale green are with dynamic conditions. Fig. 5 upward shows the fluorescence (Epi) micrographs (MGs) illustrating the used cells activity and viability for the six used segments (S1–S6); two data sets are illustrated, the downward MGs represent data carried out during five weeks, while the upward MGs represent data carried out for three days.

This enables one to have SB grafts under desire for different clinical applications. We have recently used mesodermal progenitor-cells obtained from induced pluripotent stem cells and one gets sufficiently good functional bone tissue [21–24]; this has been obtained with a biomimetic technique. In the present work, an equivalent technique could be used to produce repeatable, productive and effective SB grafts. The

quality and reproducibility of produced bone-tissue depend on how many cells affect the building processes and how these cells are spatially distributed through the scaffolds. This affects the migration, communication and differentiation, the quality and the regenerative characters of produced bone. Hinderliter et al. [103] have reported that cell-seeding processes is highly affected by the scaffold design, the segment-size and its constitution. So, in order to get high quality products, the cell-seeding and culturing processes on scaffolds should be optimized, controlled and standardized; in fact, this is a very important demand in order to attain sufficiently good BGs with high reproducibility characters to be cultured in both laboratory and clinical scales.
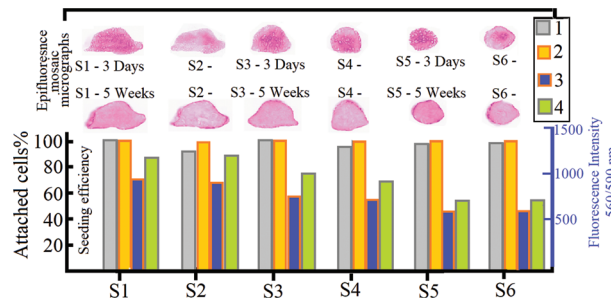

Figure 5: *DOWN:* Attached cells percentage (seeding efficiency-left) *UPWARD:* Fluorescence (Epi) micrographs (MGs) for the six used segments (S1–S6)

Sectioning of BS deficiency reorganizations into well disk-shaped design permits one to standardize the seeding protocol, to perform operant and to create repeatable growth of BGs for BS reorganization. Figs. 4A and 4B illustrate that one has obtained a homogeneous distribution of seeded-cells independent on size and/or design of the scaffolds when seeded the cells on scaffolds with the present technique. In addition, Table 2 shows the number of seeded-cells and the size of the utilized cells-suspension/BS, which has been maintained consistent. After five weeks, Fig. 6c shows that the seeding processes in the bio-incubator is by far efficient with more active-cells comparing with seeded-cells which has been seeded in static-conditions, while Fig. 6A illustrates that the dynamic system is more effective when one treats larger BGs.

Table 2: Shows the values of standard glycation concentration of some healthy individuals $G_{G\text{-standard}}$ and the activation energy ΔE as a function of temperature

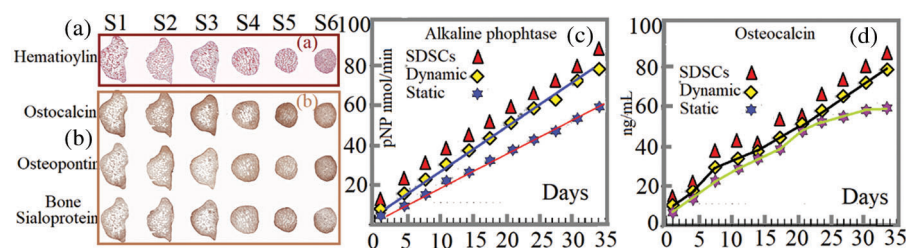| T (K)	G_G-Standard	ΔE, meV
280	0.045141	..
285	0.045513	..
290	0.045925	121
295	0.046338	117
300	0.04675	120
305	0.047163	115
310	0.047575	111
315	0.047988	97
320	0.048411	90

Figure 6: (a) Tissue generation for the 6-defect segments, (b) Immuno/histo chemical study, (c) Estimation of the alkaline phosphatese and osteoclcin liberated from BSs cultured with both static and Fig. 6, (d) Shows the same for the dynamic states

3.4 Bone-Tissue Figuration and Graft Collection

Viable tissues should be obtained when applying an adequate grow BGs in the lab with a condensed NECM assisted by the existence of one of osteonectin components. In references [21–24], we have shown that perfusion culture is very sensitive to the present approach to compact BGs from mamalian pluripotent stem cell-derived mesodermal progenitors. So, in the present work, the same osteo-inductive and perfusion issues has been used as already detailed [21–24]. Figs. 6a and 6b show good histological and immune-histo-chemical analysis of the obtained tissues.

This confirms good tissue formation through the seeding processes as proof by continuous cell penetration and formation of NECM. The quality of this formation is seen in Figs. 6a–6d which show good features of the utilized bone tissue engineering. Fig. 6c shows the effect of the release of alkaline phosphatase on the tissue formation when one has seeded cells in the bio-incubator with some comparison between static conditions, assisting the active action of interstitial movements for cell bioactivity, viability and discrimination, and tissue formation.

Fig. 6a illustrates the tissue generation for 6-defect segments, which have histological study analyzed with dynamic situations, Fig. 6b illustrates the immuno/histo chemical study of six BSs (S1–S6) cultured with dynamic situations in the bio incubator, Fig. 6c shows thw estimated data of the alkaline phosphatese and osteoclcin liberated from BSs cultured with both static and dynamic states; experimental results act for averages ± standard deviation (n = 3, Student's t-test, $P < 0.04$;) red triangles and SDSCs stand for significant difference to static conditions.

Fig. 6d illustrates the effect of the release of osteocalcin on the tissue formation when one has seeded cells in the bio-incubator with some comparison between static conditions, assisting the active action of interstitial movements for cell activity and differentiation, and tissue formation. One can notice that homogeneous BT-formation is found when using dynamic conditions; this happens independent on the BT shape, design or/and size. This reflects the significance of protocol control for the advantageous and repeatable production of BT-engineered grafts. Gathering of tinny BT-modules leads to the formation of segmental grafts with low integrity and weak design-capability. However, different authors [103–109] have tried to scale up of BTGs. Moreover, sectioning of segmental defect reconstructions leads to the formation of BT-modules that can be gathered into segmental grafts with high efficiency and low mechanical instability. Generally, bio-adaptable BT-adhesives or orthopedic sets can be utilized to give enough mechanical powerful and keep the alignment of the BT-modules when one uses the present technique-scenario along healing and/or reconstruction. It is worth noting that the present technique-scenario can, in addition, promote more developments *in vitro* pre-vascularization systems.

3.5 Statistical Analysis

Two types of statistical-analysis tools have been used in order to address the best mean value and here one can present two questions: the first concerns tests for statistical significance; and the second is addressed by measures of association. We will carry out our statistical-analysis using the first one. This type answers the question: what is the probability that what we think is a relationship between two variables is really just a chance occurrence? Therefore, the statistical analysis has been carried out with the aid of Prism6: version6.0e. Moreover, Student's *t*-examination has been used to compare between the six groups. The data are presented as means and ±SDs. We have estimated the values being statistically significant if the *P* value has been attained a value inferior to 5%

4 Conclusions

Different bone tissue (BT) engineering techniques have been used during the few past decades; however, these techniques cannot fulfil the clinical needs for various BT-engineering scenarios. The present work has fulfilled clinical application technique with different issues combined with suitable devices to close up the clinical needs. One can use the proposed technique with high multifaceted sides, ease implementation, and real improvement to the property of life patients who suffer from SB defects.

Conflicts of Interest: The authors declare that they have no conflicts of interest to report regarding the present study.

References

1. Tonk, H., Shoushrah, S. H., Babczyk, P., El Khaldi-Hansen, B., Schulze, M. et al. (2022). Treatments for osteoporosis—Which combination of pills is the best among the bad? *International Journal of Molecular Sciences, 23(3),* 1393. DOI 10.3390/ijms23031393.

2. Wei, K., Qu, Y., Gao, Y., Ma, Y. (2021). Comparison of efficacy of teriparatide (parathyroid hormone 1–34) alone and in combination with zoledronic acid for osteoporosis in postmenopausal women. *Journal of College of Physicians and Surgeons Pakistan, 31(2),* 240–242. DOI 10.29271/jcpsp.2021.02.240.

3. Kim, J. M., Lin, C., Stavre, Z., Greenblatt, M. B., Shim, J. H. (2020). Osteoblast-osteoclast communication and bone homeostasis. *Cells, 9(9),* 2073. DOI 10.3390/cells9092073.

4. Shimizu, T., Arita, K., Murota, E., Hiratsuka, S., Fujita, R. et al. (2021). Effects after starting or switching from bisphosphonate to romosozumab or denosumab in Japanese postmenopausal patients. *The Journal of Bone and Mineral Metabolism, 39(5),* 868–875. DOI 10.1007/s00774-021-01226-1.

5. Chen, X., Wang, Z., Duan, N., Zhu, G., Schwarz, E. et al. (2018). Osteoblast-osteoclast interactions. *Connective Tissue Research, 59(2),* 99–107. DOI 10.1080/03008207.2017.1290085.

6. Arias, C. F., Herrero, M. A., Echeverri, L. F., Oleaga, G. E., López, J. M. (2018). Bone remodeling: A tissue-level process emerging from cell-level molecular algorithms. *PLoS One, 13(9),* 0204171. DOI 10.1371/journal.pone.0204171.

7. Mi, J., Xu, J. K., Yao, Z., Yao, H., Li, Y. et al. (2022). In topics in osteoporosis, implantable electrical stimulation at dorsal root ganglions accelerates osteoporotic fracture healing via calcitonin gene-related peptide. *Advanced Sciences, 9(1),* e2103005. DOI 10.1002/advs.202103005.

8. Parra-Torres, A. Y., Valdés-Flores, M., Orozco, L., Velázquez-Cruz, R. (2013). Molecular aspects of bone remodeling. In: Valdés-Flores, M. (Ed.), *Topics in osteoporosis*. DOI 10.5772/54905.

9. Shetty, S., Kapoor, N., Bondu, J. D., Thomas, N., Paul, T. V. (2016). Bone turnover markers: Emerging tool in the management of osteoporosis. *Indian Journal of Endocrinology and Metabolism, 20(6),* 846–852. DOI 10.4103/2230-8210.192914.

10. Pereira, A. R., Lipphaus, A., Ergin, M., Salehi, S., Gehweiler, D. et al. (2021). Modeling of the human bone environment: Mechanical stimuli guide mesenchymal stem cell-extracellular matrix interactions. *Materials, 14(16),* 4431. DOI 10.3390/ma14164431.

11. Huzum, B., Puha, B., Necoara, R. M., Gheorghevici, S., Puha, G. et al. (2021). Biocompatibility assessment of biomaterials used in orthopedic devices: An overview (Review). *Experimental and Therapeutic Medicine, 22(5),* 1315. DOI 10.3892/etm.2021.10750.

12. Koons, G. L., Diba, M., Mikos, A. G. (2020). Materials design for bone-tissue engineering. *Nature Reviews Materials, 5(8),* 584–603. DOI 10.1038/s41578-020-0204-2.

13. Annamalai, R. T., Hong, X., Schott, N. G., Tiruchinapally, G., Levi, B. et al. (2019). Injectable osteogenic microtissues containing mesenchymal stromal cells conformally fill and repair critical-size defects. *Biomaterials, 208(3),* 32–44. DOI 10.1016/j.biomaterials.2019.04.001.

14. ReportLinker (2021). Bone Grafts and Substitutes Market by Type, Material Type, Application-Global Opportunity Analysis and Industry Forecast, 2020–2030. https://www.researchandmarkets.com/reports/5206327/bone-grafts-andsubstitutes-market-by-type.

15. Archunan, M. W., Petronis, S. (2021). Bone grafts in trauma and orthopaedics monitoring. *Cureus, 13(9),* e17705. DOI 10.7759/cureus.17705.

16. van der Stok, J., van Lieshout, E. M., El-Massoudi, Y., van Kralingen, G. H., Patka, P. (2011). Bone substitutes in the Netherlands–A systematic literature review. *Acta Biomaterialia, 7(2),* 739–750. DOI 10.1016/j.actbio.2010.07.035.

17. Reyna-Urrutia, V. A., González-González, A. M., Rosales-Ibáñez, R. (2022). Compositions and structural geometries of scaffolds used in the regeneration of cleft palates: A review of the literature. *Polymers, 14(3),* 547. DOI 10.3390/polym14030547.

18. AlMalki, F. A., Hassan, A. M., Klaab, Z. M., Abdulla, S., Pizzi, A. (2021). Tannin nanoparticles (NP99) enhances the anticancer effect of tamoxifen on ER$^+$ breast cancer cells. *Journal of Renewable Materials, 9(12),* 2077–2092. DOI 10.32604/jrm.2021.016173.

19. Fraga-Corral, M., Otero, P., Cassani, L., Echave, J., Garcia-Oliveira, P. et al. (2021). Traditional applications of tannin rich extracts supported by scientific data: Chemical composition, bio-availability and bio-accessibility. *Foods, 10(2),* 251. DOI 10.3390/foods10020251.

20. Wedaïna, A. G., Pizzi, A., Nzie, W., Danwe, R., Konai, N. et al. (2021). Performance of unidirectional biocomposite developed with piptadeniastrum africanum tannin resin and urena lobata fibers as reinforcement. *Journal of Renewable Materials, Scrivener Publishing, 9(3),* 477–493. DOI 10.32604/jrm.2021.012782.

21. Yang, Y., Abdalla, S., Scaffolds of Macro (2021). Porous tannin spray with human-induced pluripotent stem cells. *Frontiers in Bioengineering and Biotechnology, 8,* 951. DOI 10.3389/fbioe.2020.00951.

22. Abdalla, S., Al-Marzouki, F., Pizzi, A., Bahabri, F. (2018). *Bone graft with a tannin-hydroxyapatite scaffold and stem cells for bone engineering.* U.S. Patent Number: 10155069. Washington DC: U.S. Patent and Trademark Office.

23. Pizzi, A. (2019). Tannins: Prospectives and actual industrial applications. *Biomolecules, 9(8),* 344. DOI 10.3390/biom9080344.

24. Abdalla, S., Pizzi, A., Bahabri, F. S. (2020). Macro porous tannin spray-dried powder scaffolds with stem cells for bone engineering. *Materials Chemistry and Physics, 239(3),* 121980. DOI 10.1016/j.matchemphys.2019.121980.

25. Liu, F., Xu, J., Wu, L., Zheng, T., Han, Q. et al. (2021). The influence of the surface topographical cues of biomaterials on nerve cells in peripheral nerve regeneration: A review. *Stem Cells International, 2021(1),* 1–13, 8124444. DOI 10.1155/2021/8124444.

26. Calvi, L. M., Adams, G. B., Weibrecht, K. W., Weber, J. M., Olson, D. P. et al. (2003). Osteoblastic cells regulate the haematopoietic stem cell niche. *Nature, 425(6960),* 841–846. DOI 10.1038/nature02040.

27. Yin, T., Li, L. (2006). The stem cell niches in bone. *Journal of Clinical Investigations, 116(5),* 1195–1201. DOI 10.1172/JCI28568.

28. Wallace, J. M., Chen, Q. S., Fang, M., Erickson, B., Orr, B. G. et al. (2010). Multiscale analysis of morphology and mechanics in tail tendon from the ZDSD rat model of type 2 diabetes. *Langmuir, 26(10),* 7349–7354. DOI 10.1021/la100006a.

29. Wallace, J. M., Erickson, B., Les, C. M., Orr, B. G., Holl, M. M. B. (2010). Distribution of type I collagen morphologies in bone: Relation to estrogen depletion. *Bone, 46(5),* 1349– 1354. DOI 10.1016/j.bone.2009.11.020.

30. Stevens, M. M., George, J. H. (2005). Exploring and engineering the cell surface interface. *Science, 310,* 1135. DOI 10.1126/science.1106587.

31. Bettinger, C. J., Langer, R., Borenstein, J. T. (2009). Engineering substrate topography at the micro-and nanoscale to control cell function. *Angewandte Chemie International Edition, 48(3),* 5406–5415. Online Library. DOI 10.1002/anie.200805179.

32. Kumar, A., Placone, J. K., Engler, A. J. (2017). Understanding the extracellular forces that determine cell fate and maintenance. *Development, 144(23),* 4261–4270. DOI 10.1242/dev.158469.

33. Donnelly, H., Dalby, M. J., Salmeron-Sanchez, M., Sweeten, P. E. (2018). Current approaches for modulation of the nanoscale interface in the regulation of cell behavior. *Nano-Medicine, Nanotechnology, Biology and Medicine, 14(7),* 2455–2464. DOI 10.1016/j.nano.2017.03.020.

34. Dalby, M. J., Gadegaard, N., Oreffo, R. O. (2014). Harnessing, nano-topography and integrin-matrix interactions to influence stem cell fate. *Nature Materials, 13(6),* 558–569. DOI 10.1038/nmat3980.

35. Wen, J. H., Vincent, L. G., Fuhrmann, A., Choi, Y. S., Hribar, K. C. et al. (2014). Interplay of matrix stiffness and protein tethering in stem cell differentiation. *Nature Materials, 13(10),* 979–987. DOI 10.1038/nmat4051.

36. Discher, D. E., Mooney, D. J., Zandstra, P. W. (2009). Growth factors, matrices, and forces combine and control stem cells. *Science, 324(5935),* 1673–1677. DOI 10.1126/science.1171643.

37. de Peppo, G. M., Agheli, H., Karlsson, C., Ekström, K., Brisby, H. (2014). Osteogenic response of human mesenchymal stem cells to well-defined nanoscale topography *in vitro*. *International Journal of Nano-medicine, 22(9),* 2499–2515. DOI 10.2147/IJN.S58805.

38. Wang, P. Y., Bennetsen, D. T., Foss, M., Ameringer, T., Thissen, H. et al. (2015). Modulation of human mesenchymal stem cell behavior on ordered tantalum nano topographies fabricated using colloidal lithography and glancing angle deposition. *ACS Applied Materials Interfaces, 7(8),* 4979–4989. DOI 10.1021/acsami.5b00107.

39. Guven, S., Chen, P., Inci, F., Tasoglu, S., Erkmen, B. et al. (2015). Multiscale assembly for tissue engineering and regenerative medicine. *Trends Biotechnology, 33(5),* 269–279. DOI 10.1016/j.tibtech.2015.02.003.

40. Zhang, S., Holmes, T., Lockshin, C., Rich, A. (1993). Spontaneous assembly of a self-complementary oligopeptide to form a stable macroscopic membrane. *Proceedings National Academy of Science USA, 90(8),* 3334–3338. DOI 10.1073/pnas.90.8.3334.

41. Zhou, G., Tian, A., Yi, X., Fan, L., Shao, W. et al. (2021). Study on a 3D-bioprinted tissue model of self-assembled nanopeptide hydrogels combined with adipose-derived mesenchymal stem cells. *Frontiers Bioengineering Biotechnology, 3(9),* 663120. DOI 10.3389/fbioe.2021.663120.

42. Amores de Sousa, M. C., Rodrigues, C. A. V., Ferreira, I. A. F., Diogo, M. M., Linhardt, R. J. et al. (2020). Functionalization of electrospun nanofibers and fiber alignment enhance neural stem cell proliferation and neuronal differentiation. *Frontiers Bioengineering Biotechnology, 26(8),* 580135. DOI 10.3389/fbioe.2020.580135.

43. Tsou, Y. H., Khoneisser, J., Huang, P. C., Xu, X. (2016). Hydrogel as a bioactive material to regulate stem cell fate. *Bioactive Materials, 1(1),* 39–55. DOI 10.1016/j.bioactmat.2016.05.001.

44. Dellatore, S. M., Garcia, A. S., Miller, W. M. (2008). Mimicking stem cell niches to increase stem cell expansion. *Current Opinion Biotechnology, 19(5),* 534–540. DOI 10.1016/j.copbio.2008.07.010.

45. Tian, X., Yuan, X., Feng, D., Wu, M., Yuan, Y. et al. (2020). *In vivo* study of polyurethane and tannin-modified hydroxyapatite composites for calvarial regeneration. *Journal of Tissue Engineering, 11(36),* 1–9. DOI 10.1177/2041731420968030.

46. da Câmara, P. C. F., Balaban, R. C., Hedayati, M. H., Popat, K. C., Martins, A. F. et al. (2019). Novel cationic tannin/glycosaminoglycan-based polyelectrolyte multilayers promote stem cells adhesion and proliferation. *RCA Advances, (44),* 25836–25846. DOI 10.1039/C9RA03903A 2019.

47. Koopmann, A. K., Schuster, C., Torres-Rodríguez, J., Kain, S., Pertl-Obermeyer, H. et al. (2020). Tannin-based hybrid materials and their applications: A review. *Molecules, 25(21),* 4910. DOI 10.3390/molecules25214910.

48. Hernes, P. J., Hedges, J. I. (2004). Tannin signatures of barks, needles, leaves, cones, and wood at the molecular level. *Geochimica et Cosmochimica Acta, 68(6),* 1293–1307. DOI 10.1016/j.gca.2003.09.015.

49. Arbenz, A., Avérous, L. (2014). Synthesis and characterization of fully bio based aromatic polyols-oxybutylation of condensed tannins towards new macromolecular architectures. *RSC Advances, 4(106),* 61564–61572. DOI 10.1039/C4RA10691A.

50. Arbenz, A., Avérous, L. (2015). Chemical modification of tannins to elaborate aromatic bio based macromolecular architectures. *Green Chemistry, 17(5),* 2626–2646. DOI 10.1039/C5GC00282F.

51. Grishechko, L. I., Amaral-Labat, G., Szczurek, A., Fierro, V., Kuznetsov, B. N. et al. (2013). New tannin-lignin aerogels. *Industrial Crop Production, 41,* 347–355. DOI 10.1016/j.indcrop.2012.04.052.

52. Quideau, S., Deffieux, D., Douat-Casassus, C., Pouységu, L. (2011). Plant polyphenols: Chemical properties, biological activities, and synthesis. *Angewandte Chemie International, 50(3),* 586–621. DOI 10.1002/anie.201000044.

53. Falcão, L., Araújo, M. (2011). Tannins characterization in new and historic vegetable tanned leathers fibres by spot tests. *Journal Culture Heritage, 12(2),* 149–156. DOI 10.1016/j.culher.2010.10.005.

54. Tondi, G., Petutschnigg, A. (2015). Middle infrared (ATR FT-MIR) characterization of industrial tannin extracts. *Industrial Crop Production, 65(9),* 422–428. DOI 10.1016/j.indcrop.2014.11.005.

55. Shirmohammadli, Y., Efhamisisi, D., Pizzi, A. (2018). Tannins as a sustainable raw material for green chemistry: A review. *Industrial Crop Production, 126,* 316–332. DOI 10.1016/j.indcrop.2018.10.034.

56. Khanbabaee, K., van Ree, T. (2001). Classification and definition. *Natural Product Reports, 18(6),* 641–649. DOI 10.1039/b101061l.

57. Pizzi, A. (2021). Covalent and ionic bonding between tannin and collagen in leather making and shrinking: A MALDI-ToF study. *Journal of Renewable Materials, 9(8),* 1345–1364. DOI 10.32604/jrm.2021.015663.

58. Bacelo, H. A., Santos, S. C., Botelho, C. M. (2016). Tannin-based biosorbents for environmental applications–A review. *Chemical Engineering Journal, 303,* 575–587. DOI 10.1016/j.cej.2016.06.044.

59. Pasch, H., Pizzi, A., Rode, K. (2001). MALDI-TOF mass spectrometry of poly-flavonoid tannins. *Polymer, 42(18),* 7531–7539. DOI 10.1016/S0032-3861(01)00216-6.

60. Schofield, P., Mbugua, D., Pell, A. (2001). Analysis of condensed tannins: A review. *Animal Feed Science and Technology, 91(1–2),* 21–40. DOI 10.1016/S0377-8401(01)00228-0.

61. Fraga-Corral, M., García-Oliveira, P., Pereira, A. G., Lourenço-Lopes, C., Jimenez-Lopez, C. et al. (2020). Technological application of tannin-based extracts. *Molecules, 25,* 614. DOI 10.3390/molecules25030614.

62. Li, J., Li, B., Zhang, J., Zhou, X. (2019). Tannin resins for wood preservatives: A review. *Research and Application of Materials Science, 1,* 45–48. DOI 10.33142/msra.v1i1.667.

63. Ogata, T., Morisada, S., Oinuma, Y., Seida, Y., Nakano, Y. (2011). Preparation of adsorbent for phosphate recovery from aqueous solutions based on condensed tannin gel. *Journal of Hazardous Materials, 192(2),* 698–703. DOI 10.1016/j.jhazmat.2011.05.073.

64. Slabbert, N. (1992). Plant. In: Hemingway, R. F., Lakes, P. (Eds.), *Polyphenols. Basics of life sciences.* Boston, MA, USA: Springer.

65. Santos, S., Bacelo, H. A. M., Boaventura, R. A. R., Botelho, C. M. S. (2019). Tannin-adsorbents for water decontamination and for the recovery of critical metals: Current state and future perspectives. *Biotechnology Journal, 14(12),* e1900060. DOI 10.1002/biot.201900060.

66. Pizzi, A. (2008). Tannins: Major sources, properties and applications. In: *Monomers, polymers and composites from renewable resources,* pp. 179–199. Amsterdam: The Netherlands: Elsevier.

67. Braghiroli, F., Fierro, V., Izquierdo, M. T., Parmentier, J., Pizzi, A. et al. (2012). Nitrogen-doped carbon materials produced from hydrothermally treated tannin. *Carbon, 2012(50),* 5411–5420. DOI 10.1016/j.carbon.2012.07.027.

68. Hashida, K., Makino, R., Ohara, S. (2009). Amination of pyrogallol nucleus of condensed tannins and related polyphenols by ammonia water treatment. *Holzforschung, 63(3),* 319–326. DOI 10.1515/HF.2009.043.

69. Braghiroli, F., Fierro, V., Pizzi, A., Rode, K., Radke, W. et al. (2013). Reaction of condensed tannins with ammonia. *Industrial Crop Production, 44(4),* 330–335. DOI 10.1016/j.indcrop.2012.11.024.

70. Triplett, R. G., Schow, S. R. (1996). Autologous bone grafts and endosseous implants: Complementary techniques. *Journal of Oral and Maxillofacial Surgery, 54(4),* 486–494. DOI 10.1016/S0278-2391(96)90126-3.

71. Houk, C. J., Beltran, F. O., Grunlan, M. A. (2021). Suitability of EtO sterilization for poly dopamine-coated, self-fitting bone scaffolds. *Polymer Degradation and Stability, 194(1),* 109763. DOI 10.1016/j.polymdegradstab.2021.109763.

72. Bhandary, M., Hegde, A. M., Shetty, R., Shetty, P. (2021). Augmentation of narrow anterior alveolar ridge using autogenous block onlay graft in a pediatric patient: A case report. *International Journal of Clinical Pediatric Dentistry, 14(2),* 311–314. DOI 10.5005/jp-journals-10005-1931.

73. Ma, G., Wu, C., Shao, M. (2021). Simultaneous implant placement with autogenous onlay bone grafts: A systematic review and meta-analysis. *International Journal of Implant Dentistry, 7(1),* 61. DOI 10.1186/s40729-021-00311-4.

74. Hollinger, J. O., Winn, S., Bonadio, J. (2000). Options for tissue engineering to address challenges of the aging skeleton. *Tissue Engineering, 2000(6),* 341–350. DOI 10.1089/107632700418065.

75. Papantoniou, I., Hall, G. N., Lesage, N. R., Herpelinck, T., Mendes, L. et al. (2021). Turning nature's own processes into design strategies for living bone implant bio manufacturing: A decade of developmental engineering. *Advanced Drug Delivery Reviews, 169,* 22–39. DOI 10.1016/j.addr.2020.11.012.

76. U.S. Markets for Orthopedic Biomaterials for Bone Repair and Regeneration (2013). MedTech Insight: Bedminster, NJ, USA. https://pharmastore.informa.com/product/u-s-markets-for-orthopedic-biomaterials-for-bone-repair-and-regeneration/.

77. GlobeNewswire (2021). Regenerative Medicine Market Research Report: By Type (Cell Therapy, Gene Therapy, Tissue Engineered Products), Application (Musculoskeletal, Wound Care, Oncology, Dental, Ocular)-Global Industry Analysis and Demand Forecast to 2030. https://www.globenewswire.com/news-release/2021/06/01/2239389/28124/en/Worldwide-Regenerative-Medicine-Industry-to-2030-Market-Analysis-and-Demand-Forecasts.html.

78. Albert, A., Leemrijse, T., Druez, V., Delloye, C., Cornu, O. (2006). Are bone auto-grafts still necessary in 2006? A three-year retrospective study of bone grafting. *Acta Orthopaedica Belgica Orthop, 72,* 734–740.

79. https://www.stratovan.com/blog/how-convert-reduce-and-load-micro-ct-scans.

80. Einhorn, T. A., Gerstenfeld, L. C. (2015). Fracture healing: Mechanisms and interventions. *Nature Reviews Rheumatology, 11(1),* 45–54. DOI 10.1038/nrrheum.2014.164.

81. Liao, J., Li, J., Yang, F., Zhu, Y., Wang, H. (2022). Assisted compatibility, and balanced regulation of the mechanical, thermal, and antioxidant activity of polyvinyl alcohol-chinese bayberry tannin extract films using different di-aldehydes as cross-linkers. *Journal of Renewable Materials, 10(2),* 359–372. DOI 10.32604/jrm.2021.016335.

82. Einhorn, T. A., Gerstenfeld, L. C. (2015). Fracture healing: Mechanisms and interventions. *Nature Review Rheumatology, 11(1),* 45–54. DOI 10.1038/nrrheum.2014.164.

83. Oryan, A., Alidadi, S., Moshiri, A. (2014). Bone regenerative medicine: Classic options, novel strategies, and future directions. *Journal of Orthopaedic Surgery and Research, 9(1),* 1290. DOI 10.1186/1749-799X-9-18.

84. Li, Y., Chen, S. K., Li, L. (2015). Bone defect animal models for testing efficacy of bone substitute biomaterials. *Journal of Orthopaedic Translation, 3(3),* 95–104. DOI 10.1016/j.jot.2015.05.002.

85. Tremoleda, J. L., Khalil, M., Gompels, L. L. (2011). Imaging technologies for preclinical models of bone and joint disorders. *European Journal of Nuclear Medicine and Molecular Imaging, 1(1),* 11. DOI 10.1186/2191-219X-1-11.

86. Bigham-Sadegh, A., Oryan, A. (2015). Selection of animal models for pre-clinical strategies in evaluating the fracture healing, bone graft substitutes and bone tissue regeneration and engineering. *Connective Tissue Research, 56(3),* 175–194. DOI 10.3109/03008207.2015.1027341.

87. Lienemann, P. S., Metzger, S., Kiveliö, A. S. (2015). Longitudinal *in vivo* evaluation of bone regeneration by combined measurement of multi-pinhole SPECT and micro-CT for tissue engineering. *Scientific Reports, 5(1),* 10238. DOI 10.1038/srep10238.

88. Lee, S. W., Padmanabhan, P., Ray, P. (2009). Stem cell-mediated accelerated bone healing observed with *in vivo* molecular and small animal imaging technologies in a model of skeletal injury. *Journal of Orthopaedic Research, 27(3),* 295–302. DOI 10.1002/jor.20736.

89. Ventura, M., Franssen, G. M., Oosterwijk, E. (2014). SPECT *vs.* PET monitoring of bone defect healing and biomaterial performance *in vivo*. *Journal of Tissue Engineering and Regenerative Medicine, 10(10),* 843–854. DOI 10.1002/term.1862.

90. Ventura, M., Boerman, O. C., Franssen, G. M. (2014). Monitoring the biological effect of BMP-2 release on bone healing by PET/CT. *Journal of Controlled Release, 183,* 138–144. DOI 10.1016/j.jconrel.2014.03.044.

91. Annibali, S., Bellavia, D., Ottolenghi, L. (2013). Micro-CT and PET analysis of bone regeneration induced by biodegradable scaffolds as carriers for dental pulp stem cells in a rat model of calvarial critical size defect: Preliminary data. *Journal of Biomedical Materials Research B, 102(4),* 815–825. DOI 10.1002/jbm.b.33064.

92. Skaliczki, G., Weszl, M., Schandl, K. (2012). Compromised bone healing following spacer removal in a rat femoral defect model. *Acta Physiologica Hungarica, 99(2),* 223–232. DOI 10.1556/APhysiol.99.2012.2.16.

93. Lin, C., Chang, Y., Li, K. (2013). The use of ASCs engineered to express BMP2 or TGF-β3 within scaffold constructs to promote calvarial bone repair. *Biomaterials, 34(37),* 9401–9412. DOI 10.1016/j.biomaterials.2013.08.051.

94. Leyendecker Junior, A., Gomes Pinheiro, C. C., Lazzaretti Fernandes, T. (2018). The use of human dental pulp stem cells for *in vivo* bone tissue engineering: A systematic review. *Journal of Tissue Engineering, 9(3),* 1–18. DOI 10.1177/2041731417752766.

95. Morsczeck, C., Reichert, T. E. (2018). Dental stem cells in tooth regeneration and repair in the future. *Expert Opinion on Biological Therapy, 18(2),* 187–196. DOI 10.1080/14712598.2018.1402004.

96. Roseti, L., Parisi, V., Petretta, M., Cavallo, C., Desando, G. et al. (2017). Scaffolds for bone tissue engineering: State of the art and new perspectives. *Materials Science and Engineering: C, 78,* 1246–1262. DOI 10.1016/j.msec.2017.05.017.

97. Maliha, S. G., Lopez, C. D., Coelho, P. G., Witek, L., Cox, M. et al. (2020). Bone tissue engineering in the growing calvaria using dipyridamole-coated, three-dimensionally-printed bioceramic scaffolds. *Plastic and Reconstructive Surgery, 145(2),* 337e–347e. DOI 10.1097/PRS.0000000000006483.

98. Spanjer, E. C. K., Bittermann, G. K., van Hooijdonk, I. E., Rosenberg, A. J., Gawlitta, D. et al. (2017). Taking the endochondral route to craniomaxillofacial bone regeneration: A logical approach? *Journal of Cranio-Maxillofacial Surgery, 45(7),* 1099–1106. DOI 10.1016/j.jcms.2017.03.025.

99. Debelmas, A., Picard, A., Kadlub, N. (2018). Contribution of the periosteum to mandibular distraction. *PLoS One, 13(6),* e0199116. DOI 10.1371/journal.pone.0199116 2018.

100. Takahashi, K., Tanabe, K., Ohnuki, M., Narita, M., Ichisaka, T. et al. (2007). Induction of pluripotent stem cells from adult human fibroblasts by defined factors. *Cell, 131(5),* 861–872. DOI 10.1016/j.cell.2007.11.019.

101. Sladkova, M., Palmer, M., Öhman, C., Cheng, J., Al-Ansari, S. et al. (2017). Engineering human BGs with new macroporous calcium phosphate cement scaffolds. *Journal of Tissue Engineering and Regenerative Medicine, 2(3),* 715–726. DOI 10.1002/term.2491.

102. Bitar, M., Brown, R. A., Salih, V., Kidane, A. G., Knowles, J. C. et al. (2008). Effect of cell density on osteoblastic differentiation and matrix degradation of biomimetic dense collagen scaffolds. *Biomacromolecules, 9(1),* 129–135. DOI 10.1021/bm701112w.

103. Vunjak-Novakovic, G., Radisic, M. (2004). Cell seeding of polymer scaffolds. biopolymer methods in tissue engineering. In: *Methods in molecular biology*, pp. 131–145. Humana Press.

104. Hinderliter, P. M., Minard, K. R., Orr, G., Chrisler, W. B., Thrall, B. D. et al. (2010). A computational model of particle sedimentation, diffusion and target cell dosimetry for *in vitro* toxicity studies. *Particle and Fibre Toxicology, 7(1),* 36. DOI 10.1186/1743-8977-7-36.

105. de Peppo, G. M., Marolt, D. (2014). Make no bones about it: Cells could soon be reprogrammed to grow replacement bones? *Expert Opinion on Biological Therapy, 14(1),* 1–5. DOI 10.1517/14712598.2013.840581.

106. Takahashi, K., Tanabe, K., Ohnuki, M., Narita, M., Ichisaka, T. et al. (2007). Induction of pluripotent stem cells from adult human fibroblasts by defined factors. *Cell, 131(5),* 861–872. DOI 10.1016/j.cell.2007.11.019.

107. Chen, M., Wang, X., Ye, Z., Zhang, Y., Zhou, Y. et al. (2011). A modular approach to the engineering of a centimeter-sized bone tissue construct with human amniotic mesenchymal stem cells-laden micro-carriers. *Biomaterials, 32(30),* 7532–7542. DOI 10.1016/j.biomaterials.2011.06.054.

108. Grayson, W. L., Fröhlich, M., Yeager, K., Bhumiratana, S., Chan, M. E. et al. (2010). Engineering anatomically shaped human bone grafts. *PNAS, 107(8),* 3299–3304. DOI 10.1073/pnas.0905439106.

109. Petite, H., Viateau, V., Bensaïd, W., Meunier, A., de Pollak, C. et al. (2000). Tissue-engineered bone regeneration. *National Biotechnology, 18(9),* 959–963. DOI 10.1038/79449.